The strength of the Iceland plume: A geodynamical scaling approach

Neil M. Ribe, Paul J Tackley, Patrick Sanan

The Strength of the Iceland Plume: A Geodynamical Scaling Approach

Neil M. Ribe[1]
Laboratoire FAST, CNRS, Université Paris-Saclay,
Bâtiment 530, Campus Universitaire,
Orsay, F-91400, France

Paul J. Tackley, Patrick Sanan
Institute of Geophysics, Department of Earth Sciences, ETH Zurich,
Sonneggstrasse 5, 8092 Zürich, Switzerland

August 25, 2020

[1]Corresponding author (ribe@fast.u-psud.fr)

Abstract

An important measure of the strength of a mantle plume is its buoyancy flux B, defined as the integral over a horizontal plane of the product of the vertical velocity and the density deficit within the plume. In the case of the Iceland plume, which currently rises directly beneath the mid-Atlantic ridge, published estimates of B cover a range of a factor of 37. To reconcile these diverse estimates, we study a simple fluid mechanical model of a ridge-centered plume in which plume fluid with spreadability σ (buoyancy over viscosity) is supplied at a volumetric rate Q from a plume conduit located directly beneath a ridge with a half spreading rate U. The plume fluid spreads laterally to form a thin pool beneath a lithosphere whose thickness increases as the square root of age. Application of scaling and dimensional analysis to this model leads to a general scaling law for the 'waist width' W_w, the length of the plume-induced elevation anomaly along the ridge. The law has the form $W_w/W_0 = f_2(\Pi_b, \Pi_s)$, where $W_0 = (\sigma Q^4/U^5)^{1/6}$ is the fundamental length scale for plume-ridge interaction, $\Pi_b = (\sigma Q/U^2)^{1/3}$ is of the order of the aspect ratio (width/thickness) of the plume pool, $\Pi_s = (\kappa^2\sigma/U^3)^{1/4}$ measures the effect on the pool of the sloping base of the lithosphere (κ is the thermal diffusivity), and f_2 is an unknown function. We determine f_2 using a suite of 32 numerical solutions of a three-dimensional thermomechanical model implemented in the code StagYY (Tackley, 2008). To apply our scaling law to Iceland, we invert it to estimate the buoyancy flux B required to produce a waist width $W_w = 2300 \pm 300$ km. After correction for the effect

of ridge migration, we find $B = 2.3 \pm 0.6$ Mg s^{-1}. This is comparable within uncertainty to the buoyancy flux $B = 3.0 \pm 0.8$ Mg s^{-1} of the Hawaiian plume estimated using a 3-D dynamical model by Ribe and Christensen (1999).

keywords: mantle plumes; plume-ridge interaction; Iceland; lubrication theory

1 Introduction

The mantle plume that creates Iceland is, together with the Hawaiian plume, one of the two best known and most intensively studied of all mantle plumes. By a nice coincidence, these two plumes happen to represent the two end-member extremes of the phenomenon of plume-ridge interaction (PRI), whereby a mantle plume influences the bathymetry, geochemistry and crustal structure along a portion of a nearby mid-ocean ridge. In the Hawaiian case, the distance between the plume and the nearest ridge is so great that PRI does not occur at all. At the opposite extreme, the Iceland plume is located directly below the mid-Atlantic ridge (MAR), making this system the paradigmatic example of PRI.

Intuition tells us that the intensity of PRI should be proportional to some measure of the 'strength' of the mantle plume involved. Since the pioneering work of Sleep (1990), the most commonly used measure of plume strength is the 'buoyancy flux' B. It is defined as

$$B = \int_S w \delta\rho \mathrm{d}S, \tag{1}$$

where w is the (laterally variable) vertical velocity within the plume, $\delta\rho > 0$ is the density deficit of the plume material, and the surface integral is taken

over a horizontal cross-section of the plume. The SI units of B are kg s^{-1}, but we shall use the more customary units Mg s^{-1} = 10^3 kg s^{-1}. If the plume is in steady-state, then B will be independent of the chosen cross-section. If the plume's buoyancy is due to temperature differences alone, then $\delta\rho = \rho_0\alpha(T - T_0)$ where T is the temperature, T_0 is the temperature outside the plume, ρ_0 is the reference density at the temperature T_0 and α is the coefficient of thermal expansion. The buoyancy flux of a mantle plume is important because it is proportional to the heat flux that the plume carries. Because many of Earth's largest mantle plumes are likely to arise at the core-mantle boundary, estimating their combined buoyancy flux provides an estimate of the heat flux coming out of the core (Davies, 1988; Hoggard et al., 2020).

Two general methods have been used to estimate the buoyancy fluxes of mantle plumes interacting with mid-ocean ridges. The first, which we shall call the 'flux balance' method, is based on a balance between the vertical buoyancy flux in the plume conduit and the horizontal flux of buoyancy in the elevated topography of the hotspot swell carried by the moving plate (Sleep, 1990; Schilling, 1991). In its simplest form, the equation for this method is $B = c_1(\rho_0 - \rho_w)EUW_w$, where E is the maximum excess elevation, U is the half-spreading rate, W_w is the width of the elevation anomaly along the ridge itself, ρ_w is the density of seawater, and c_1 is a model-dependent constant of proportionality of order unity. Implicit in this method is the assumption that the negative buoyancy of the hotspot swell is in isostatic equilibrium with the positive buoyancy of the underlying low-density plume material that compensates it. An alternative version of the flux balance method (Sleep, 1990;

Schilling, 1991) equates the volumetric flux Q (rather than the buoyancy flux) of the plume with the rate at which new lithosphere of thickness H and width W_w is carried away from the ridge at the rate U. This gives $Q = c_2 HUW_w$, where c_2 is a model-dependent constant of proportionality. The volume flux thus estimated can be transformed into a buoyancy flux $B = \rho_0 \alpha \Delta T_m Q$, where ΔT_m is an assumed maximum temperature anomaly of the plume.

The second method is based on the width W_w of the excess elevation alone (Feighner and Richards, 1995; Ribe and Delattre, 1998). It simply asks how large the volume flux Q must be to generate an elevation anomaly with the observed width W_w. In view of laboratory observations that the width of a pool of buoyant plume material centered on a ridge increases in both directions away from the ridge, Feighner and Richards (1995) called W_w the 'waist width'. We shall therefore call the second method for estimating B the 'waist width' method. This method requires a dynamical model (numerical or experimental) to predict the relation between W_w and Q.

The aforementioned methods have been applied by several authors to estimate the buoyancy flux of the Iceland plume. Sleep (1990) estimated $B = 1.4$ Mg s^{-1} using a modified version of the second flux balance method described above. Schilling (1991) used both versions of the flux balance method to estimate $Q \approx 45$ m^3 s^{-1}, which corresponds to $B = 1.4$ Mg s^{-1} for his estimated excess plume temperature $\Delta T_m = 263$ K. He used a reduced waist width $W_w = 920$ km corresponding to the width of geochemical (rather than elevation) anomalies along the ridge around Iceland. Feighner and Richards (1995) used the waist width method in conjunction with laboratory experi-

ments. They proceeded indirectly by verifying that the volume flux $Q \approx 45$ m^3 s^{-1} estimated by Schilling (1991) corresponded to a waist width of 850 km according to their experimentally-based scaling law, reasonably close to the value (920 km) of Schilling (1991). Ribe and Delattre (1998) used the waist width method together with a dynamical model based on lubrication theory to conclude that a volume flux $Q = 30$ m^3 s^{-1} (corresponding to $B = 0.7 \pm 0.17$ Mg s^{-1} for $\Delta T_m = 200 \pm 50$ K) was required to explain a waist width $W_w = 920$ km. King and Adam (2014) used a geometric flux balance approach and two versions of the MiFil (minimization and filtering) method of Adam et al. (2005) to recalculate buoyancy fluxes for 54 terrestrial hotspots. Their three estimates for Iceland were 1.40 Mg s^{-1}, 1.61 Mg s^{-1} and 1.52 Mg s^{-1}. Parnell-Turner et al. (2014) used three independent flux-balance arguments to estimate $B = 18 \pm 7$ Mg s^{-1}, $B = 26 \pm 9$ Mg s^{-1} and $B = 17 \pm 5$ Mg s^{-1}, respectively. Finally, Hoggard et al. (2020) estimated $B = 4.0 \pm 1.0$ Mg s^{-1} using a flux balance argument in the context of a model in which the plume pool comprises discrete 'fingers' that spread radially away from the hotspot.

The most striking aspect of the foregoing list of estimates is the enormous range they cover, encompassing a factor of 37 from the lowest (0.7 Mg s^{-1}) to the highest (26 Mg s^{-1}). The aim of the present study is to explain and reconcile this disagreement using a geodynamical modeling approach. We begin (in § 2) by applying dimensional and scaling analysis to a simple fluid mechanical model for a ridge-centered plume, including the effects of a lithosphere that thickens with age and migration of the ridge relative to the plume. The result is a general scaling law for the waist width W_w that

involves an undetermined function of the key dimensionless parameters of the problem. Next (§ 3), we use three-dimensional thin-layer and thermomechanical numerical models to characterize the undetermined function from § 2. Finally (§ 4), we invert our scaling law for W_w to estimate the buoyancy flux ($B = 2.3 \pm 0.6$ Mg s^{-1}) required to explain the observed waist width ($W_w = 2300 \pm 300$ km) of the Iceland plume. The paper concludes (§ 5) with a discussion of our new estimate in light of previous estimates of the same quantity.

2 Dimensional and scaling analysis

To begin our study, we use a combination of dimensional and scaling analysis to determine as much as we can about how the waist width W_w depends on the various input parameters of the problem. Dimensional analysis is a generally applicable method based on the fact that a mathematical relation among a number of dimensional model parameters is equivalent to a relation among a smaller number of dimensionless combinations ('groups') of those parameters. The basic theorem of dimensional analysis, called Buckingham's Π-theorem (Buckingham, 1914), is a recipe for determining how many dimensionless groups are both necessary and sufficient for the problem at hand. Scaling analysis, by contrast, is a more specific method that starts from the differential equation(s) that govern the phenomenon of interest. By requiring the dominant terms in the equation to be of the same order of magnitude, one can determine the fundamental length and (in unsteady problems) time scales that characterize the phenomenon, and that cannot be determined by dimensional analysis alone.

To help build intuition, the following discussion proceeds step by step, considering first the idealized case of a vanishingly thin lithosphere, then a more realistic lithosphere whose thickness increases as the square root of age, and finally the effect of migration of the ridge relative to the plume.

2.1 Vanishingly thin lithosphere

Fig. 1 shows the idealized model upon which we shall base our scaling analysis. Plume material with constant viscosity η_p and density deficit $\delta\rho$ is supplied at a volumetric rate Q by a plume conduit located directly beneath a stationary ridge with half spreading rate U. The steady-state thickness of the plume material beneath the lithosphere is $h(x, y)$, and the lithosphere is assumed to have a vanishingly small thickness. The width of the plume pool is $W(x)$, and the waist width is $W_w = W(0)$.

Our starting point is the partial differential equation that governs the steady-state thickness $h(x, y)$ of the pool of buoyant plume material shown in Fig. 1. That equation can be derived using the theory of viscous flow in thin layers (lubrication theory), and is (Ribe et al., 1995; Ribe, 2018)

$$\frac{\partial}{\partial x}\psi(x,h) = \sigma\nabla^2(h^4) + \frac{Q}{\pi a^2}\exp\left(-\frac{r^2}{a^2}\right), \tag{2}$$

where

$$\psi(x,z) = \frac{2U}{\pi} z\tan^{-1}\left(\frac{x}{z}\right), \tag{3}$$

is the 'corner flow' streamfunction of the ridge-generated mantle flow (Batchelor, 1967; Ribe, 2018),

$$\sigma = \frac{g\delta\rho}{12\eta_p} \tag{4}$$

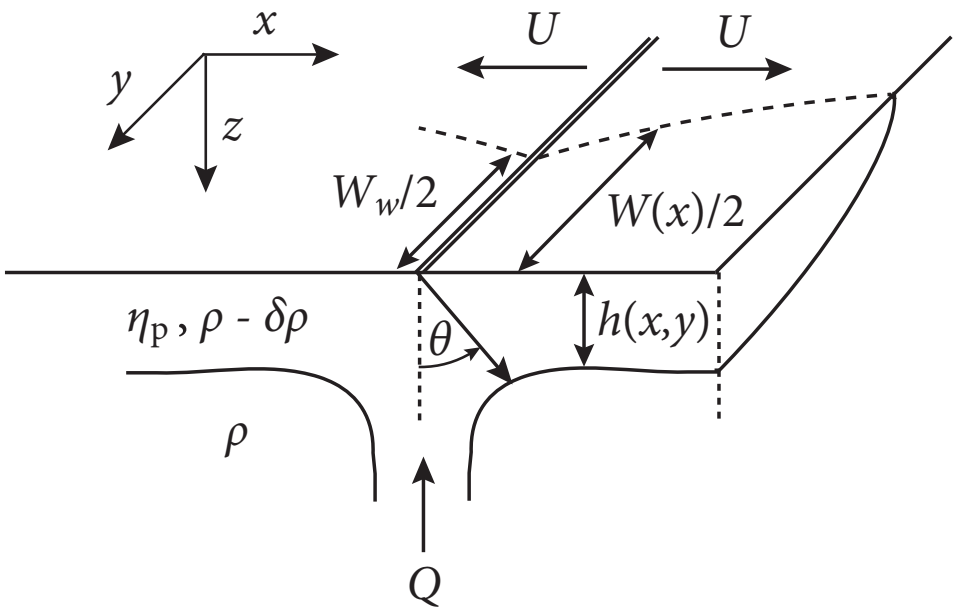

Figure 1: Lubrication model for a ridge-centered plume. Plume material with viscosity η_p and density deficit $\delta\rho$ is supplied at a volumetric rate Q beneath a stationary (non-migrating) ridge with half spreading rate U. The steady-state thickness of the pool of plume material beneath the lithosphere is $h(x, y)$, and the lithosphere is assumed to have vanishingly small thickness. The width of the pool is $W(x)$, and the waist width is $W_w = W(0)$.

is the 'spreadability' of the plume material, ∇ is the horizontal gradient operator, and r is the horizontal radial distance from the center of the plume conduit of radius a. From left to right, the terms in (2) represent advection of the plume material by the ambient flow, gravity-driven spreading of plume material, and injection of plume material into the pool, respectively. The definition (4) of σ assumes that the shear stress on the lower surface of the plume pool is zero. This boundary condition is more appropriate than a no-slip condition when the viscosity ratio (exterior/pool) is smaller than the pool's width/thickness ratio (Ribe, 2018).

The characteristic scales for the thickness $h(x, y)$ and the width $W(x)$ of the plume pool can now be determined by a scaling analysis of (2). To keep the notation simple, we shall denote these characteristic scales by the symbols h and W, respectively. There are two distinct pairs of length scales, depending on the angle θ shown in fig. 1.

The first pair of length scales applies at distances far from the ridge where $\theta \approx \pi/2$. As a preliminary, we note that the derivatives $\partial/\partial x$ and $\partial/\partial y$ both scale as W^{-1}, because the geometry of the problem does not impose different length scales in the x- and y-directions. Now far from the ridge $\tan^{-1}(x/z) \approx \pi/2$ and $(\partial/\partial x)\psi(x, h) \approx U\partial h/\partial x \sim Uh/W$, where the symbol $\sim$ means 'scales as', i.e. 'is proportional to and of the same order of magnitude as'. This term must balance the gravitational spreading term $\sigma\nabla^2(h^4)$, implying $Uh/W \sim \sigma h^4/W^2$. In addition, conservation of volume flux requires $Q \sim U_d W h$, where U_d is the downstream (x-direction) velocity of the plume pool. Because the rate of gravitational spreading in the x-direction is much smaller than the plate speed U (Ribe and Christensen,

1994), we can set $U_d = U$. Solving the two foregoing relations for h and W we find

$$W \sim \left(\frac{\sigma Q^3}{U^4}\right)^{1/4} \equiv W_1, \quad h \sim \left(\frac{Q}{\sigma}\right)^{1/4} \equiv h_1. \tag{5}$$

The scales (5) are identical to those that apply for a Hawaii-type plume rising beneath an intact (unrifted) lithosphere moving at speed U relative to the plume (Ribe and Christensen, 1994).

The second pair of lengthscales applies when $\theta \ll 1$ and $y > a$ (i.e., outside the plume conduit), in which case the ridge-generated flow is primarily vertical. Then $\tan^{-1}(x/z) \approx x/z$, and (3) implies $(\partial/\partial x)\psi(x,h) \approx U$. The balance of the advection and gravitational spreading terms in (2) then gives $U \sim \sigma h^4/W^2$. As before, conservation of volume flux requires $Q \sim UWh$. Solving these two relations for h and W we obtain

$$W \sim \left(\frac{\sigma Q^4}{U^5}\right)^{1/6} \equiv W_0, \quad h \sim \left(\frac{Q^2}{\sigma U}\right)^{1/6} \equiv h_0. \tag{6}$$

These scales were first found by Ribe (2018). Unlike the scales (5) they are specific to plume-ridge interaction. The scale W_0 corrects the erroneous lateral length scale $(Q/U)^{1/2}$ proposed by Ribe et al. (1995) and adopted by a number of subsequent authors (Feighner and Richards, 1995; Feighner et al., 1995; Ribe, 1996; Ito et al., 1997; Ribe and Delattre, 1998).

2.2 Thickening lithosphere

The simple model described in the previous subsection assumes that the lithosphere has a vanishingly small thickness. In reality, of course, the thickness of the lithosphere increases as the square root of its age. This increase has two competing dynamical effects that were not accounted for in the model

of § 2.1. First, the slope of the lithosphere-asthenosphere boundary (LAB) provides an additional gravitational driving force for upslope flow of buoyant plume material towards the ridge (Kincaid et al., 1995, 1996). This effect tends to increase the waist width. Second, and less obviously, the LAB is not a material surface. Instead, material continuously flows across it because the lithosphere's vector velocity, which is horizontal at the sloping LAB, has a small component normal to that surface. This normal component of velocity corresponds to a sink of plume material, which gets transformed into effectively rigid lithosphere as it moves across the LAB. This effect tends to decrease the waist width. (Ribe, 1996).

To quantify the physics just described, we use dimensional analysis to determine how the waist width W_w depends on the input parameters of the problem. Inspection of the lubrication equation (2) and the expression (3) for the streamfunction shows that W_w depends on σ, Q and U; the dependence on a can be neglected as long as $a \ll W_w$. In addition, W_w must depend on the thermal diffusivity κ, which together with U controls the thickening of the lithosphere. There exists therefore a functional relationship among the $M = 5$ quantities W_w, σ, Q, U and κ. Of these five quantities, $K = 2$ have independent dimensions. According to Buckingham's Π-theorem, $M - K = 3$ independent dimensionless groups can be formed from these quantities. While the groups can be chosen in an infinite number of ways, it is generally good practice to use physically meaningful definitions. The obvious choice for the first group is W_w/W_0, where W_0 is the fundamental length scale for PRI found by scaling analysis in § 2.1. As the second group, we choose the

'buoyancy number'

$$\Pi_b = \frac{W_0}{h_0} = \left(\frac{\sigma Q}{U^2}\right)^{1/3}, \tag{7}$$

which is of the order of the aspect ratio (width/thickness) of the plume pool. As the third group, we choose the ratio of the slope of the lithosphere at $x = W_0$ to the slope in the x-direction of the plume pool itself. According to the half-space cooling model the former slope is $\sim (\kappa/UW_0)^{1/2}$. The slope of the plume pool is $\sim h_0/W_0$. Taking the ratio of these slopes and using the definitions (6), we obtain the 'slope number'

$$\Pi_s = \left(\frac{\kappa^2\sigma}{U^3}\right)^{1/4}. \tag{8}$$

Putting everything together, we expect the waist width W_w of a ridge-centered plume beneath a thickening lithosphere to obey a scaling law having the general form

$$\frac{W_w}{W_0} = f_2\left(\Pi_b, \Pi_s\right) \tag{9}$$

where f_2 is an undetermined function that remains to be found.

2.3 Effect of ridge migration

The last physical factor influencing the waist width is the speed U_m at which the ridge is migrating relative to the hotspot. Ridge migration of course implies that the distance between the plume conduit and the ridge is constantly changing; here we are interested only in the instant in time when the plume conduit is directly beneath the ridge.

The most obvious dimensionless group to use to characterize the effect of ridge migration is the ratio Π_m of the ridge migration speed to the half

spreading rate, which we call the 'migration number':

$$\Pi_m = \frac{U_m}{U}. \tag{10}$$

Therefore when the ridge is migrating, the waist width of a ridge-centered plume must follow a scaling law having the general form

$$\frac{W_w}{W_0} = f_3\left(\Pi_b, \Pi_s, \Pi_m\right) \tag{11}$$

where f_3 is an unknown function. It is related to the function f_2 previously introduced by $f_3(\Pi_b, \Pi_s, 0) = f_2(\Pi_b, \Pi_s)$.

3 Numerical models

The general scaling laws for the waist width derived in the previous section involve undetermined functions f_2 and f_3 of the dimensionless groups Π_b, Π_s and Π_m. The appearance of an undetermined function is typical whenever a scaling law involves more than a single dimensionless group, as in our case. In general, the form of the function is not simple and cannot be determined by dimensional or scaling analysis; instead, laboratory experiments or explicit solutions of a numerical model are necessary. Accordingly, this section is devoted to characterizing the functions f_2 and f_3 numerically. For clarity, the exposition is organized under the same headings as in the previous section. However, a section entitled 'Vanishly thin lithosphere' is absent because we jump directly to the more realistic case of a thickening lithosphere.

3.1 Thickening lithosphere

As shown in § 2.2, the scaling law for the waist width in the presence of a thickening lithosphere involves the undetermined function $f_2(\Pi_b, \Pi_s)$. The

definition (8) of the dimensionless group Π_s contains the thermal diffusivity κ. This suggests that we should use a 3-D thermomechanical model to determine the function f_2. The model we use here builds on a series of previous 3-D convection models of ridge-centered plumes and of the Iceland plume more specifically (Ribe et al., 1995; Ito et al., 1996, 1999; Albers and Christensen, 2001; Ruedas et al., 2004; Marquart et al., 2007; Gallego et al., 2013). However, our approach differs from most of these earlier ones in that it uses a large suite of numerical solutions to determine a quantitative scaling law.

Accordingly, in this subsection we study a 3-D convection model of a ridge-centered plume implemented in the code StagYY (Tackley, 2008). The details of the numerical implementation are outlined in Appendix A. Briefly, the domain of the solution is a Cartesian box 400 km deep and of variable length and width. The ridge flow is generated by a spreading velocity $U_{\mathrm{spread}}(x) = U \tanh(x/b)$ imposed on the upper surface, where $b = 25$ km is a small transition width. The ridge-centered plume is generated by a Gaussian temperature anomaly $\Delta T \exp[-(x^2 + y^2)/a^2]$ imposed on the bottom of the box. In most of the solutions presented below, the rheology is Newtonian and the viscosity obeys a standard Arrhenius law with realistic activation parameters. For each steady-state solution obtained, the spreadability σ and the volume flux Q are calculated as described in Appendix A.

Fig. 2 shows an example of a solution for reference values of the temperature anomaly $\Delta T = 225$ K, plume radius $a = 55$ km, and half spreading rate $U = 3.1$ cm yr^{-1}. The buoyancy flux of the plume is $B = 1.17$ Mg s^{-1}. Fig. 2a shows the temperature field in the symmetry plane $y = 0$, and fig. 2b shows the 'isostatic topography' $\zeta(x, y)$, which is proportional at each point

to the vertical integral over the depth of the box of the temperature anomaly associated with the plume (Appendix A).

Note that both Π_s and Π_b depend on the spreadability σ, which in turn depends on the characteristic plume viscosity η_p. We identify η_p with η_m, the minimum viscosity over the whole model domain. In practice this definition picks out the viscosity in the hottest central part of the plume beneath the 'hotspot' $(x, y) = (0, 0)$.

To test the scaling law (9), we obtained 32 steady-state numerical solutions with different values of ΔT, a and U. The results are collected in fig. 3, which shows the normalized waist width $W_w/W_0 \equiv f_2$ (colored squares) as a function of Π_b and Π_s. The points (Π_b, Π_s) are irregularly distributed because Π_b and Π_s are model outputs, not inputs. The colors vary smoothly over the Π_b-Π_s plane, showing that all the data points collapse onto a single two-dimensional surface even though three parameters (ΔT, a and U) were varied to obtain them. Fig. 3 thus confirms the validity of the scaling law (9).

Another important feature of fig. 3 is that the scaled waist width W_s/W_0 decreases as the slope number Π_s increases. To understand why, recall (§ 2.2) that the sloping base of the lithosphere has two competing dynamical effects: it enhances upslope flow of plume material, which tends to increase the waist width, and it represents a sink of plume material, which tends to decrease the waist width. The results of fig. 3 show that the second of these effects is the dominant one.

For the convenience of readers who may wish to use the scaling law shown in fig. 3, we provide in Appendix C the coefficients of a bicubic polynomial

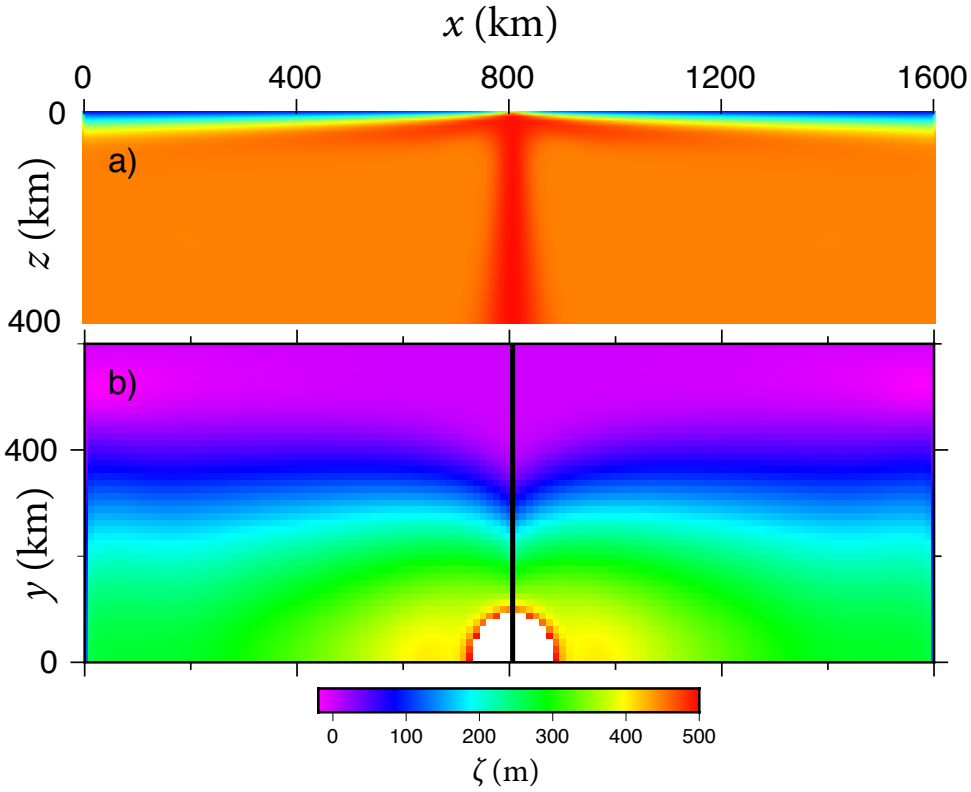

Figure 2: Three-dimensional steady-state numerical solution for a ridge-centered plume with reference values of the temperature anomaly $\Delta T = 225$ K, plume radius $a = 55$ km, and half spreading rate $U = 3.1$ cm yr^{-1}. The buoyancy flux of the plume is $B = 1.17$ Mg s^{-1}. (a) Temperature anomaly in the vertical symmetry plane $y = 0$. (b) Isostatic topography $\zeta(x, y)$ (see Appendix A for definition). The vertical black line shows the location of the ridge. White indicates a region where $\zeta > 500$ m.

fit of the function $f_2(\Pi_s, \Pi_b)$.

It is of some interest to examine how non-Newtonian (dislocation creep) rheology influences the scaling law we have determined. The composite Newtonian/non-Newtonian rheological law we used is specified by (20) and (21). It involves a reference stress τ_0 at which the diffusion creep and dislocation creep viscosities are the same. For the parameters of the solution shown in fig. 2, we found that the addition of non-Newtonian rheology has essentially no effect on the waist width for $\tau_0 = 10$ MPa, and increases it by only 7.5% for $\tau_0 = 0.3$ MPa. The smallness of this effect is somewhat surprising, because the flow just beneath the ridge should be controlled primarily by the non-Newtonian viscosity due to the high strain rates there. The smallness of the effect is probably due to the smoothing of the velocity singularity at the ridge by the finite transition width b, and by the fact that we impose a miminum cutoff viscosity $\eta_{\min} = 10^{17}$ Pa s. In any case, the small effect of non-Newtonian rheology justifies our decision to consider only Newtonian rheology in the solutions used to construct fig. 3.

3.2 Effect of ridge migration

As shown in § 2.3, the scaling law for the waist width in the presence of ridge migration involves an undetermined function $f_3(\Pi_b, \Pi_s, \Pi_m)$. Because it is impractical to characterize completely a function of three arguments, we opted for the simpler approach of estimating the magnitude of the ridge migration effect for an Iceland-type plume. Our first attempt was to use StagYY with $a = 68$ km, $\Delta T = 275$ K and $U = 3.96 \times 10^{-10}$ m s^{-1}. The code was first run for 60 Ma with a fixed ridge to give the plume time to

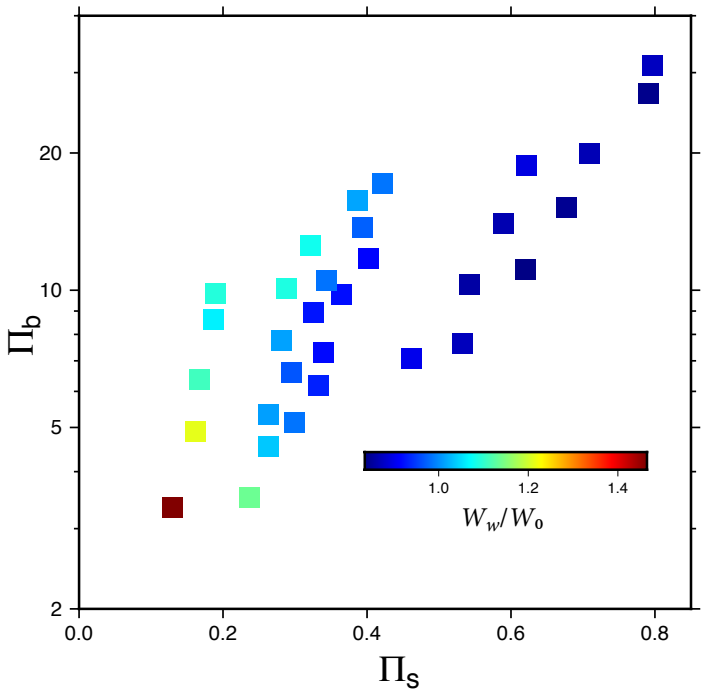

Figure 3: Normalized waist width $W_w/W_0 \equiv f_2$ as a function of the slope number Π_s and buoyancy number Π_b for 32 numerical solutions for a steady ridge-centered plume with different values of the half spreading rate U, the temperature anomaly ΔT, and the plume radius a.

develop 1200 km away from the ridge, after which the ridge migration speed was ramped up during 20 Ma to $U_m = 1.5U$. However, we found that the buoyancy flux of the plume diminished by more than a factor of ten before increasing again when the ridge was close to the plume, an unrealistic result that is probably an artefact of the model boundary conditions. We therefore decided to use a simpler model that contains the basic physics, namely an extended version of the lubrication model of § 2.1 with ridge migration added. The extended lubrication equation is

$$\frac{\partial h}{\partial t} + \frac{\partial}{\partial x}\psi(x,h) = \sigma\nabla^2(h^4) + \frac{Q}{\pi a^2}\exp\left(-\frac{r^2}{a^2}\right), \tag{12a}$$

$$r^2 = (x - x_0 + U_m t)^2 + y^2. \tag{12b}$$

Equation (12) differs from the simpler lubrication equation (2) by the addition of an unsteady term $\partial h/\partial t$ and by a new expression for r that includes relative motion between the plume and the ridge. Equation (12) with the expression (3) for $\psi(x,z)$ is valid for a lithosphere of vanishing thickness, which is of course unrealistic. However, we anticipate that this should not matter much because we are only interested here in a relative effect, i.e. the factor by which ridge migration changes the waist width. For convenience, (12) is solved in the reference frame of the ridge, in which the plume moves toward the ridge with velocity $-U_m\mathbf{e}_x$, where $\mathbf{e}_x$ is a unit vector in the x-direction. The position of the plume at the beginning of the simulation $t = 0$ is $x = x_0$.

Fig. 4 shows the results for $\Pi_b = 25$, a typical buoyancy number for an Iceland-sized plume. Fig. 4a shows the steady-state thickness $h(x,y)$ of the plume pool for a non-migrating ridge directly above the plume source, while Fig. 4b shows $h(x,y,t_0)$ with a migrating ridge with $\Pi_m = 1.23$, at

the instant $t = t_0$ when the ridge is directly above the plume source. The waist width for the latter case is smaller than that for a steady ridge-centered plume by 17%. This decrease of the waist width due to ridge migration has a simple physical explanation. During the time when the ridge is approaching the plume, the lithosphere above the plume is moving relative to it not at speed U, but rather at the enhanced speed $U + U_m$. This greater relative speed corresponds to stronger advection of the plume pool, which counteracts gravitational spreading more effectively and makes the pool narrower than it would be in the absence of ridge migration (Ribe and Delattre, 1998).

4 Strength of the Iceland plume

We now use the 'waist width' method to obtain a new estimate of the buoyancy flux of the Iceland plume by inverting our scaling law $W_w/W_0 = f_2(\Pi_s, \Pi_b)$ for a ridge-centered plume. Our first task is to choose a range of values of W_w appropriate for the Iceland plume. Fig. 5 shows the axial elevation of the Mid-Atlantic Ridge as function of distance from Iceland. Based on these data we choose $W_w = 2300 \pm 300$ km as the representative width of the ridge elevation anomaly associated with Iceland. The maximum and minimum values in this range are shown in fig. 5 by horizontal arrows. Our chosen range is consistent with the value $W_w = 2400$ km assumed by Parnell-Turner et al. (2014). Moreover, the lower end of the range (= 2000 km) corresponds to twice the distance from Iceland of the transition between smooth and rough crust along the Reykjanes ridge, which is a possible proxy for the waist width (N. White, personal communication).

Turning next to our scaling law, we first note that the relevant portion

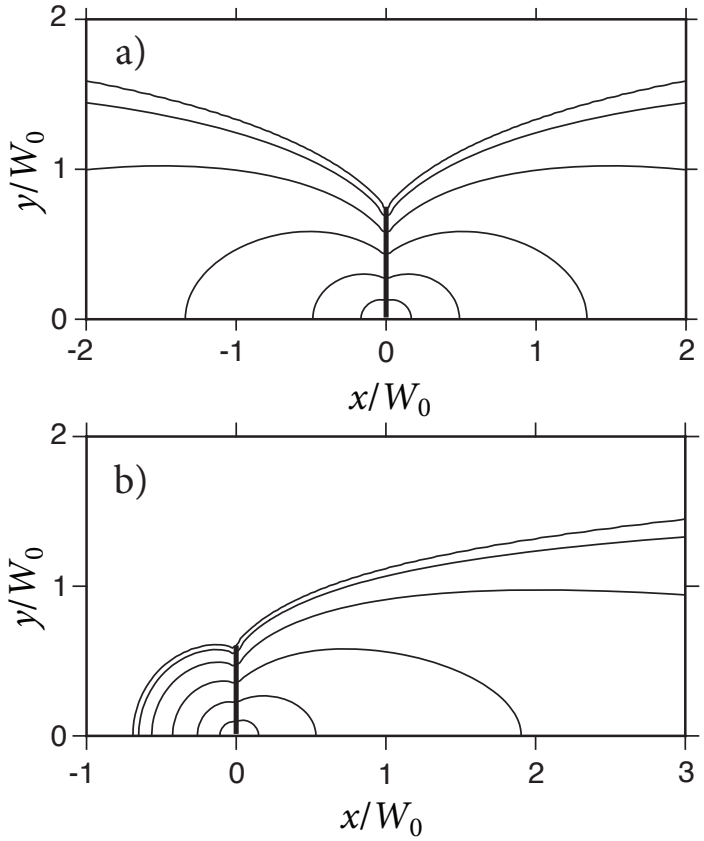

Figure 4: Effect of ridge migration on the waist width W_w for a plume directly beneath a ridge, as predicted by the lubrication model with $\Pi_b = 25$ and a lithosphere of vanishing thickness. (a) Contour plot of steady-state plume pool thickness $h(x, y)$ for a plume source directly beneath a stationary ridge. The contour interval is $0.05h_0$ and the outermost contour is $0.05h_0$. The position of the ridge is $x = 0$, and the thick vertical line has length $W_w/2$. (b) Same as (a), but with ridge migration at speed $1.23U$ to the right relative to the plume stem.

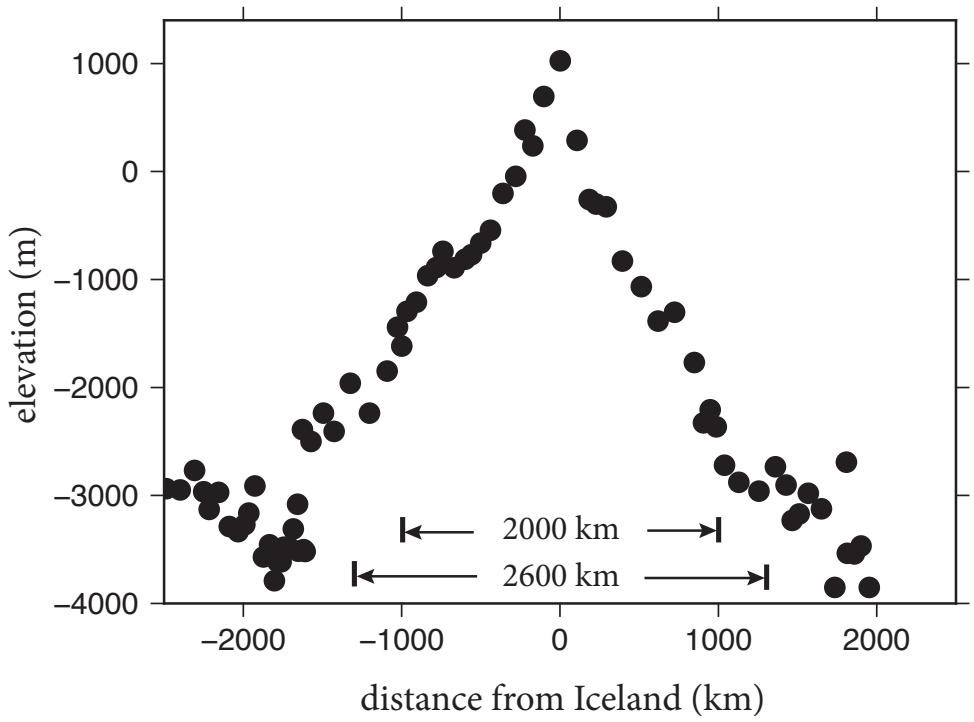

Figure 5: Axial elevation of the mid-Atlantic Ridge as a function of distance from Iceland. Negative distances are south of Iceland. Data courtesy of C. Dalton (personal communication).

of the Π_s-Π_b space for the Iceland plume is the upper right corner of fig. 3, as we shall verify *a posteriori*. Using the average of the values of W_w/W_0 for the two points closest to that corner, we obtain the scaling law

$$W_w = 0.86 W_0. \tag{13}$$

Solving (13) for $B \equiv \alpha \rho_0 \Delta T_m Q$, we obtain

$$B = 1.25 \alpha \rho_0 \Delta T_m \left(\frac{W_w^6 U^5}{\sigma} \right)^{1/4}. \tag{14}$$

We use a value $U = 2.85 \times 10^{-10}$ m s^{-1} (0.90 cm yr^{-1}) calculated in Appendix B from the plate rotation vectors of model HS3-NUVEL1A of Gripp and Gordon (2002). Next, we calculate σ at the depth z_m where the viscosity within the plume is a minimum, and where the plume's excess temperature is ΔT_m. Using (21), we find

$$\sigma = \frac{g \alpha \rho_0 \Delta T_m}{12 \eta_m}, \quad \eta_m = \eta_0 \exp \left[\frac{E_1 + g \rho_0 z_m V_1}{R(T_0 + \Delta T_m)} - \frac{E_1}{R T_0} \right] \tag{15}$$

In (15), the quantities g, ρ_0, α, η_0, E_1, V_1, R and T_0 are all known constants. From our numerical solutions, we find $z_m = 25$ km.

Fig. 6 shows the buoyancy flux predicted by (14) as a function of the (unknown) excess plume temperature ΔT_m, for three values of W_w in the range 2000-2600 km. The buoyancy flux ranges from 1.54 ± 0.30 Mg s^{-1} for $\Delta T_m = 120$ K to 1.84 ± 0.36 Mg s^{-1} for $\Delta T_m = 260$ K.

The foregoing estimates of B were predicted by a scaling law for a steady ridge-centered plume, and do not take into account the progressive migration of the mid-Atlantic ridge relative to the Iceland plume during the past several tens of Ma. As we noted earlier, the importance of ridge migration can be characterized by a dimensionless 'migration number' $\Pi_m = U_m/U$, where U_m

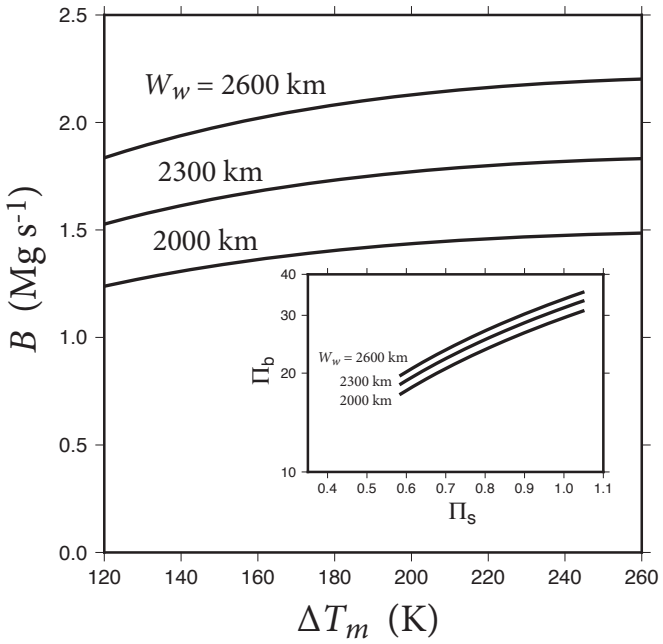

Figure 6: Predicted buoyancy flux B of the Iceland plume as a function of the plume's excess temperature ΔT_m, for three values of the waist width W_w. B is calculated from (14) as described in the text. Inset: values of Π_s and Π_b corresponding to the curves in the main figure. ΔT_m increases from 120 K to 260 K from lower left to upper right along each curve.

is the ridge migration speed. In Appendix B we use the HS3-NUVEL1A plate rotation vectors to estimate $\Pi_m = 1.23$ for the Iceland plume/ridge system. As we explained at the end of § 3.2, the effect of ridge migration is to reduce the waist width (by 17% for the case considered in § 3.2) relative to the case without ridge migration. This means that in the presence of ridge migration a greater buoyancy flux is required to explain a given value of the waist width.

The results of fig. 4 allow us to determine the factor by which the buoyancy flux B must be increased to compensate for the effect of ridge migration. Let $W_w^{\rm est}$ be some estimated value of the waist width. Then in view of the definition (6) of the length scale W_0, the scaling law $W \propto W_0$ can be written in two ways as

$$W_w^{\rm est} = 1.464\beta Q_{\rm no\ migr}^{2/3} = 1.209\beta Q_{\rm migr}^{2/3} \tag{16}$$

where $\beta = (\sigma/U^5)^{1/6}$ and the subscripts 'migr' and 'no migr' indicate values with and without ridge migration, respectively. The constants 1.464 and 1.209 that appear in (16) are the values of the waist width in units of W_0 from Figs. 4a and 4b, respectively. Now $B \propto Q$, whence (16) implies

$$\frac{B^{\rm migr}}{B^{\rm no\ migr}} = \left(\frac{1.464}{1.209}\right)^{3/2} = 1.33. \tag{17}$$

This result means that the estimated values of B in Fig. 6 must be increased by 33% to account for the effects of ridge migration that were neglected in constructing that figure. Taking into account this enhancement factor and the uncertainty of the temperature excess ΔT_m, we obtain our final estimate $B = 2.3 \pm 0.6$ Mg s^{-1} for the buoyancy flux of the Iceland plume.

5 Discussion

In § 2.1 we noted that our plume-ridge interaction lengthscale $(\sigma Q^4/U^5)^{1/6} \equiv W_0$ corrects an erroneous length scale $(Q/U)^{1/2} \equiv S_0$ proposed by Ribe et al. (1995). However, that does not mean that previous studies using the length scale S_0 (Ribe et al., 1995; Ribe, 1996; Ribe and Delattre, 1998) are incorrect. The reason is that S_0 and W_0 are simply related by $S_0 = W_0 \Pi_b^{-1/2}$, where Π_b is the buoyancy number (7). Thus one can use S_0 as the basic length scale as long as one takes the buoyancy number systematically into account. The difference is essentially one of economy: scaling laws expressed in terms of the correct lengthscale W_0 will be simpler and cleaner than laws expressed in terms of S_0, which will involve an extra dependence on Π_b.

Our estimate $B = 2.3 \pm 0.6$ Mg s^{-1} for the buoyancy flux of the Iceland plume differs from most previous estimates of this quantity, being intermediate between lower values (Sleep, 1990; Schilling, 1991; Ribe and Delattre, 1998; King and Adam, 2014) and much higher ones (Parnell-Turner et al., 2014). Most of the lower values are within the narrow range 1.4-1.6 Mg s^{-1}. These estimates are almost certainly too low because the underlying models assume $W_w = 800$-920 km. Such widths are appropriate for the geochemical anomalies along the mid-Atlantic Ridge around Iceland, but do not reflect the much larger width of the elevation anomaly evident in fig. 5.

We now examine the much larger estimates of B obtained by Parnell-Turner et al. (2014). We focus on the second and third of their three estimates because equations for these cases are either given by the authors or can easily

be inferred. Their second estimate is

$$B_2 = \pi d^2 U \rho_0 \alpha \Delta T_m \tag{18}$$

where $d = W_w/2$ is the radius of a plume pool assumed to be circular. Using $U = 1.25$ cm yr^{-1}, $d = 1200$ km, $\rho_0 = 3200$ kg m^{-3}, $\alpha = 3 \times 10^{-5}$ K^{-1} and $\Delta T_m = 150$ K, we obtain $B_2 = 26$ Mg s^{-1}, the value cited by Parnell-Turner et al. (2014). However, we note the appearance in (18) of the product of the half-spreading rate U and the planform area πd^2 of the plume pool. It seems to us more realistic to replace the quantity $\pi d^2 U$ by $2dh(2U)$, the product of the cross-sectional area of a plume pool with thickness h and the full spreading rate $2U$ (to account for flux of material away from the ridge in both directions). Our estimate of the buoyancy flux is therefore obtained from that of Parnell-Turner et al. (2014) by multiplying it by $4h/\pi d \equiv \chi_2$. To estimate h, we use the scale h_0 defined by (6) with $Q = 110$ m^3 s^{-1} and $\sigma = 4.5 \times 10^{-17}$ m^{-1} s^{-1}, values obtained directly from one of our 3-D numerical simulations of an Iceland-sized plume. We thereby find $h = 94$ km. This yields $\chi_2 = 0.10$, which implies a reduced estimate $B_2 = 2.6$ Mg s^{-1} of the buoyancy flux. This new value is within the range 2.3 ± 0.6 Mg s^{-1} that we estimated based on our scaling law.

The third estimate of Parnell-Turner et al. (2014) is

$$B_3 = \pi d^2 h \rho_0 \alpha \Delta T_m / \tau \tag{19}$$

where $\tau = 30$ Ma is the time required to fill a plume pool of volume $\pi d^2 h$. With the values of d, h, ρ_0 α and ΔT_m given above, (19) gives the estimate $B_3 = 17$ Mg s^{-1} of Parnell-Turner et al. (2014) if one assumes $h = 250$ km. However, using our more realistic value $h = 94$ km we find $B_3 = 6.5$ Mg s^{-1}.

This estimate is 60% lower than that of Parnell-Turner et al. (2014), but still more than twice the value $B = 2.9$ Mg s^{-1} at the upper end of our range.

The most recent estimate $B = 4.0 \pm 1.0$ Mg s^{-1} of the buoyancy flux of the Iceland plume is that of Hoggard et al. (2020), based on a model in which the plume pool comprises a small number of discrete fingers of thickness z_a that spread radially to a maximum distance R_{max}. Upon neglecting two smaller terms in eqn. (3) of Hoggard et al. (2020), that expression for the volume flux becomes $Q = 3\pi z_a R_{max}^2 / 8\Delta t$, where $\Delta t = 15$ Ma is the time (estimated from the geometry of the V-shaped ridges south of Iceland) required for pulses of hot material to spread down the length of a finger. The most striking aspect of the foregoing formula is that it is independent of the (half-) spreading rate U. This makes the model of Hoggard et al. (2020) fundamentally different than the fluid-mechanical models investigated in the present study, for which $Q \propto U^{5/4}$ (eqn. (14)).

Finally, it is of interest to compare our estimated buoyancy flux for the Iceland plume with corresponding estimates for the Hawiian plume. The classic estimates $B_{\mathrm{Hawaii}} = 6.3$ Mg s^{-1} (Davies, 1988) and 8.7 Mg s^{-1} (Sleep, 1990) are based on equating the vertical flux of buoyancy in the plume stem to the horizontal flux of buoyancy associated with the topography anomaly of the Hawaiian swell moving 'downstream' to the NW with a speed equal to the plate speed. Vidal and Bonneville (2004) used a similar flux balance method to estimate B_{Hawaii} as a function of time; for the past 15 Ma, they found values in the ranges 2.5-4.4 Mg s^{-1} and 3.9-6.4 Mg s^{-1} for two different lithospheric subsidence models. As mentioned earlier, King and Adam (2014) used three versions of the flux balance method to estimate the buoy-

ancy fluxes of 54 terrestrial hotspots, and found values $B_{\mathrm{Hawaii}} = 4.66$ Mg s^{-1}, 7.1 Mg s^{-1}, and 4.9 Mg s^{-1}. However, the classical flux balance approach does not take into account the fact that plume material moves downstream at an average speed that is lower than the plate speed, due to the presence of shear in the asthenosphere (Ribe and Christensen, 1994). Nor does it allow for the additional buoyancy due to the depleted residuum of melting, which compensates a significant portion of the swell topography (Ribe and Christensen, 1999). Ribe and Christensen (1999) presented a 3-D thermomechanical model that includes both these effects, and estimated the buoyancy flux of the Hawaiian plume by fitting the present-day melt production rate and the width and amplitude of the Hawaiian swell. They thereby found $B_{\mathrm{Hawaii}} = 3.0 \pm 0.8$ Mg s^{-1}. We prefer this estimate to the others cited above because the underlying dynamical model is more physically realistic. Provisionally accepting this estimate, we conclude that the buoyancy fluxes of the Iceland and Hawaiian plumes are comparable given the uncertainties involved.

Acknowledgements. We thank N. White for helpful discussions and generous advice, and C. Dalton for kindly providing her ridge elevation data. Detailed and constructive reviews by R. Katz and H. Schmeling helped greatly to improve the original manuscript. This work was supported by grant BFC 221950 from the Progamme National de Planétologie (PNP) of the Institut des Sciences de l'Univers (INSU) of the CNRS, France.

A Numerical implementation

The code StagYY (Tackley, 2008) employs a finite-volume discretization and a multigrid solver to determine inertia-free flow in a fluid with variable viscosity. It can handle both Newtonian (diffusion creep) and non-Newtonian (dislocation creep) rheologies. While most of our numerical solutions used Newtonian rheology, a few used a composite diffusion creep/dislocation creep rheology. In this more general case, the viscosity is

$$\eta = \left(\frac{1}{\eta_1} + \frac{1}{\eta_{3.5}} \right)^{-1}, \tag{20}$$

where η_1 is the Newtonian viscosity (rheological power-law index $n = 1$) and $\eta_{3.5}$ is the non-Newtonian viscosity ($n = 3.5$; Bai et al., 1991). The general expression for both viscosities is

$$\eta_n = \eta_0 \left(\frac{\tau}{\tau_0} \right)^{1-n} \exp\left(\frac{E_n + pV_n}{RT} - \frac{E_n}{RT_0} \right) \tag{21}$$

where $\eta_0 = 10^{19}$ Pa s is a reference viscosity, τ is the second invariant of the deviatoric stress, τ_0 is a reference deviatoric stress, E_n is the activation energy, p is the pressure, V_n is the activation volume, R is the universal gas constant, and $T_0 = 1600$ K is the temperature of the mantle well below the cooling lithosphere. We used the values of E_n and V_n for dry olivine given in Table 1 of Karato and Wu (1993).

The input parameters that specify a given numerical solution are the plume temperature anomaly ΔT, the plume radius a and the half-spreading rate U. The ranges used were 180 K $\leq \Delta T \leq$ 275 K, 35 km $\leq a \leq$ 66 km, and 4×10^{-10} m s$^{-1} \leq U \leq 3 \times 10^{-9}$ m s^{-1}. The horizontal dimension of each finite volume was 12.5 km for all runs. The vertical grid was refined near the

top and bottom of the model domain, the average finite volume height being 12.5 km.

Turning to the boundary conditions, we recall that the velocity boundary condition on the upper surface that drives the ridge flow and the thermal boundary condition on the bottom that drives the plume were given in § 3.1. The two vertical boundaries normal to $\mathbf{y}$ are planes of mirror symmetry. The bottom boundary and the two vertical boundaries normal to $\mathbf{x}$ are permeable with zero shear stress but some resistance to normal flow. The normal stress σ_{nn} on these boundaries is related to the normal velocity u_n by $\sigma_{nn} = \eta u_n / D$, where η is the viscosity and D is a virtual boundary distance (Ribe and Christensen, 1994). We used $D = 500$ km for the bottom boundary and $D = 2600$ km for the side boundaries.

For each numerical solution corresponding to a given set of values of ΔT, a and U, we calculated several output parameters as follows.

The first output parameter is the isostatic topography, defined as

$$\zeta(x, y) = \frac{\rho_0 \alpha}{\rho_0 - \rho_w} \int_0^h \delta T(x, y, z) \mathrm{d}z, \tag{22}$$

where x is the horizontal coordinate perpendicular to the ridge, y is the coordinate parallel to the ridge, and z is the depth. In (22), $\rho_0 = 3300$ kg m^{-3} is the mantle density, $\rho_w = 1000$ kg m^{-3} is the density of seawater, $\alpha = 3.5 \times 10^{-5}$ K^{-1} is the thermal expansivity, $h = 400$ km is the depth of the model box, and δT is the local temperature anomaly due to the presence of the plume. It is defined as $\delta T = T(x, y, z) - T(x, y_{\max}, z)$ where $y_{\max}$ is the width of the model box, chosen to be sufficiently large that the plume does not influence the temperature on the vertical plane $y = y_{\max}$.

The second output parameter is the waist width W_w, which is defined as (twice) the value of y at which the isostatic topography along the ridge falls below 30 m.

A third output parameter is the buoyancy flux B of the plume defined as

$$B = -\rho_0 \alpha \int \mathbf{u} \cdot \mathbf{e}_z (T - T_0) \mathrm{d}x \mathrm{d}y. \tag{23}$$

where $\mathbf{e}_z$ is a downward-pointing vertical unit vector and the integral is over the bottom of the model box.

A fourth output parameter is the minimum viscosity η_m in the plume directly beneath the hotspot $(x, y) = (0, 0)$. Let T_m be the temperature at the point where the viscosity is η_m.

The aforementioned output parameters are sufficient for calculating the volume flux Q and the spreadability σ, which are in turn needed to calculate the plume width scale W_0 and the dimensionless parameters Π_b and Π_s. We calculated the volume flux as

$$Q = \frac{B}{\rho_0 \alpha \Delta T_m}, \tag{24}$$

where $\Delta T_m = T_m - T_0$. The spreadability was calculated as

$$\sigma = \frac{g \rho_0 \alpha \Delta T_m}{12 \eta_m}. \tag{25}$$

Note that Q and σ are calculated using the temperature T_m and the viscosity η_m at the point where the viscosity is minimum, because that point corresponds best to the point at which the plume fluid is injected into the pool. Once Q and σ are known, the length scale W_0 and the buoyancy number Π_b were calculated using (24), (25) and the input value of U. Finally, the slope number Π_s was calculated assuming $\kappa = 7.6 \times 10^{-7}$ m^2 s^{-1}.

B Rates of spreading and ridge migration at Iceland

In this appendix we estimate the half-spreading rate U and the ridge migration speed U_m for the mid-Atlantic ridge at Iceland, where the North American plate (plate 1) and the Eurasian plate (plate 2) meet. Let $\mathbf{n}$ be the unit normal vector to the ridge pointing from plate 1 to plate 2, and let $\mathbf{U}_1$ and $\mathbf{U}_2$ be the velocities of plates 1 and 2 in the hotspot reference frame. Then

$$U = \frac{1}{2}\left|(\mathbf{U}_2 - \mathbf{U}_1)\cdot\mathbf{n}\right|, \quad U_m = \frac{1}{2}\left|(\mathbf{U}_2 + \mathbf{U}_1)\cdot\mathbf{n}\right|. \tag{26}$$

To estimate $\mathbf{U}_1$ and $\mathbf{U}_2$, we use the angular velocities of model HS3-NUVEL1A, found in Table 12 of Gripp and Gordon (2002). It is most convenient to use a mixture of spherical and Cartesian coordinates. The radial unit vector is

$$\mathbf{r} = \cos\theta\,\mathbf{z} + \sin\theta(\cos\phi\,\mathbf{x} + \sin\phi\,\mathbf{y}), \tag{27}$$

where θ is the colatitude, ϕ is the longitude, and $\mathbf{x}$, $\mathbf{y}$ and $\mathbf{z}$ are Cartesian unit vectors in the directions indicated. Transforming the angular velocities from HS3-NUVEL1A into Cartesian coordinates, we have

$$\boldsymbol{\omega}_1 = 5.443\ 10^{-17}\mathbf{x} + 1.297\ 10^{-17}\mathbf{y} - 2.046\ 10^{-16}\mathbf{z}, \tag{28a}$$

$$\boldsymbol{\omega}_2 = 1.517\ 10^{-17}\mathbf{x} + 5.112\ 10^{-17}\mathbf{y} - 9.987\ 10^{-17}\mathbf{z}, \tag{28b}$$

in units of radians s^{-1}. Next, we note that the center of Iceland is located approximately at 65° N latitude and 341.5° E longitude. The radial vector from the center of the Earth to this point is

$$\mathbf{R}_0 = 2.553\ 10^{6}\mathbf{x} - 8.543\ 10^{5}\mathbf{y} + 5.774\ 10^{6}\mathbf{z} \tag{29}$$

610 in units of m. Noting now that $\mathbf{U}_j = \boldsymbol{\omega}_j \times \mathbf{R}_0$, we find

$$\mathbf{U}_1 = -9.992\ 10^{-11}\mathbf{x} - 8.366\ 10^{-10}\mathbf{y} - 7.961\ 10^{-11}\mathbf{z} \tag{30a}$$

611

$$\mathbf{U}_2 = 2.098\ 10^{-10}\mathbf{x} - 3.426\ 10^{-10}\mathbf{y} - 1.435\ 10^{-10}\mathbf{z} \tag{30b}$$

612 in units of m s^{-1}.

613 The final step is to determine the normal vector $\mathbf{n}$. To estimate the
614 strike of the ridge, we use the line connecting the southernmost point of the
615 Kolbeinsey Ridge at 66.65° N latitude and 340.5° E longitude (point $\mathbf{R}_+$)
616 and the northernmost point of the Reykjanes Ridge at 64.1° N latitude and
617 337.5° E longitude (point $\mathbf{R}_-$). In Cartesian coordinates,

$$\mathbf{R}_+ = 2.380\ 10^6\mathbf{x} - 8.429\ 10^5\mathbf{y} + 5.849\ 10^6\mathbf{z}, \tag{31a}$$

618

$$\mathbf{R}_- = 2.571\ 10^6\mathbf{x} - 1.065\ 10^6\mathbf{y} + 5.731\ 10^6\mathbf{z}. \tag{31b}$$

619 Now the three components of $\mathbf{n}$ satisfy the three simultaneous equations
620 $(\mathbf{R}_+ - \mathbf{R}_-) \cdot \mathbf{n} = (\mathbf{R}_+ + \mathbf{R}_-) \cdot \mathbf{n} = \mathbf{n} \cdot \mathbf{n} - 1 = 0$. The solution is

$$\mathbf{n} = 0.6956\mathbf{x} + 0.6948\mathbf{y} - 0.1829\mathbf{z}. \tag{32}$$

621 Substituting (30) and (32) into (26), we obtain

$$U = 2.85\ 10^{-10}\ \text{m s}^{-1}\ (0.90\ \text{cm yr}^{-1}) \tag{33a}$$

622

$$U_m = 3.51\ 10^{-10}\ \text{m s}^{-1}\ (1.11\ \text{cm yr}^{-1}). \tag{33b}$$

C Regression for the waist width of a ridge-centered plume

We represent the function $f_2(\Pi_s, \Pi_b)$ shown in fig. 3 by a bicubic polynomial of the form

$$f_2 = \sum_{i=0}^{3} \sum_{j=0}^{3-i} c_{ij} (\Pi_s)^i (\log_{10} \Pi_b)^j. \tag{34}$$

Using a standard least-squares procedure, we find that the coefficients that provide the best fit to the 32 points in fig. 3 are

$$c_{00} = 3.306, \quad c_{01} = -4.852, \quad c_{02} = 4.733, \quad c_{03} = -2.223, \tag{35a}$$

$$c_{10} = -3.916, \quad c_{11} = -1.096, \quad c_{12} = 7.000, \quad c_{20} = 7.922, \tag{35b}$$

$$c_{21} = -16.72, \quad c_{30} = 8.685 \tag{35c}$$

The RMS error of the fit is 0.028. Note that (34)-(35) is only reliable for points (Π_s, Π_b) that lie within the 'cloud' of points in fig. 3, and should not be used to extrapolate to points lying outside the cloud.

References

Adam, C., Vidal, V., and Bonneville, A. 2005. MiFil: A method to characterize seafloor swells with application to the south central Pacific. *Geochem. Geophys. Geosyst.*, **6**, Q01003.

Albers, M., and Christensen, U. R. 2001. Channeling of plume flow beneath mid-ocean ridges. *Earth Planet. Sci. Lett.*, **187**, 207–220.

Bai, Q., Mackwell, S. J., and Kohlstedt, D. L. 1991. High-temperature creep of olivine single crystals, 1. Mechanical results for buffered samples. *J. Geophys. Res.*, **96**, 2441–2463.

Batchelor, G. K. 1967. *An Introduction to Fluid Dynamics*. Cambridge: Cambridge University Press.

Buckingham, E. 1914. On physically similar systems; illustrations of the use of dimensional equations. *Phys. Rev.*, **4**, 345–376.

Davies, G. F. 1988. Ocean bathymetry and mantle convection 1. Large-scale flow and hotspots. *J. Geophys. Res.*, **89**, 10,467–10,480.

Feighner, M., and Richards, M. A. 1995. The fluid dynamics of plume-ridge and plume-plate interactions: An experimental investigation. *Earth Planet. Sci. Lett.*, **129**, 171–182.

Feighner, M. A., Kellogg, L. H., and Travis, B. J. 1995. Numerical modeling of chemically buoyant mantle plumes at spreading ridges. *Geophys. Res. Lett.*, **22**, 715–718.

Gallego, A., Ito, G., and Dunn, R. A. 2013. Investigating seismic anisotropy beneath the Reykjanes Ridge using models of mantle flow, crystallographic evolution, and surface wave propagation. *Geochem. Geophys. Geosyst.*, **14**, 3250–3267.

Gripp, A. E., and Gordon, R. G. 2002. Young tracks of hotspots and current plate velocities. *Geophys. J. Int.*, **150**, 321–361.

Hoggard, M. J., Parnell-Turner, R., and White, N. 2020. Hotspots and mantle plumes revisited: Towards reconciling the mantle heat transfer discrepancy. *Earth Planet. Sci. Lett.*, **542**, 116317.

Ito, G., Lin, J., and Gable, C. W. 1996. Dynamics of mantle flow and melting at a ridge-centered hotspot: Iceland and the Mid-Atlantic Ridge. *Earth Planet. Sci. Lett.*, **144**, 53–74.

Ito, G., Lin, J., and Gable, C. 1997. Interaction of mantle plumes and migrating midocean ridge systems: Implications for the Galapagos plume-ridge system. *J. Geophys. Res.*, **102**, 15403–15417.

Ito, G., Shen, Y., Hirth, G., and Wolfe, C. J. 1999. Mantle flow, melting, and dehydration of the Iceland mantle plume. *Earth Planet. Sci. Lett.*, **165**, 81–96.

Karato, S.-I., and Wu, P. 1993. Rheology of the upper mantle: A synthesis. *Science*, **260**, 771–778.

Kincaid, C., Ito, G., and Gable, C. 1995. Laboratory investigation of the interaction of off-axis mantle plumes and spreading centres. *Nature*, **376**, 758–761.

Kincaid, C., Schilling, J.-G., and Gable, C. 1996. The dynamics of off-axis plume-ridge interaction in the uppermost mantle. *Earth Planet. Sci. Lett.*, **137**, 29–43.

King, S. D., and Adam, C. 2014. Hotspot swells revisited. *Phys. Earth Planet. Int.*, **235**, 66–83.

Marquart, G., Schmeling, H., and Cadek, O. 2007. Dynamic models for mantle flow and seismic anisotropy in the North Atlantic region and comparison with observations. *Geochem. Geophys. Geosyst.*, **8**, Q02008.

Parnell-Turner, R., White, N., Henstock, T., Murton, B., Maclellan, J., and Jones, S. M. 2014. A continuous 55-million-year record of transient mantle plume activity beneath Iceland. *Nature Geosci.*, **7**, 914–919.

Ribe, N. M. 1996. The dynamics of plume-ridge interaction, 2. Off-ridge plumes. *J. Geophys. Res.*, **101**, 16,195–16,204.

Ribe, N. M. 2018. *Theoretical Mantle Dynamics*. Cambridge University Press.

Ribe, N. M., and Christensen, U. 1994. Three-dimensional modeling of plume-lithosphere interaction. *J. Geophys. Res.*, **99**, 669–682.

Ribe, N. M., and Christensen, U. 1999. The dynamical origin of Hawaiian volcanism. *Earth Planet. Sci. Lett.*, **171**, 517–531.

Ribe, N. M., and Delattre, W. L. 1998. The dynamics of plume-ridge interaction-III. The effects of ridge migration. *Geophys. J. Int.*, **133**, 511–518.

Ribe, N. M., Christensen, U. R., and Theissing, J. 1995. The dynamics of plume-ridge interaction, 1: Ridge-centered plumes. *Earth Planet. Sci. Lett.*, **134**, 155–168.

Ruedas, T., Schmeling, H., Marquart, G., Kreutzmann, A., and Junge, A. 2004. Temperature and melting of a ridge-centred plume with application to Iceland. Part I: Dynamics and crust production. *Geophys. J. Int.*, **158**, 729–743.

Schilling, J.-G. 1991. Fluxes and excess temperatures of mantle plumes inferred from their interaction with migrating mid-ocean ridges. *Nature*, **352**, 397–403.

Sleep, N. H. 1990. Hotspots and mantle plumes: Some phenomenology. *J. Geophys. Res.*, **95**, 6715–6736.

Tackley, P. J. 2008. Modelling compressible mantle convection with large viscosity contrasts in a three-dimensional spherical shell using the yin-yang grid. *Phys. Earth Planet. Int.*, **171**, 7–18.

Vidal, V., and Bonneville, A. 2004. Variations of the Hawaiian hot spot activity revealed by variations in the magma production rate. *J. Geophys. Res.*, **109**, B03104.